WM9 **3:46 pm**

Novel optically transparent add/drop node for use in high-speed packet-switched networks

N. M. Rijnders, A. C. van Bochove, *Department of Electrical Engineering, University of Twente, P.O. Box 217, 7500 AE Enschede, The Netherlands*

Optical switching nodes that are transparent to wavelength, bit-rate, and modulation format can be exploited to obtain an increased and efficient use of the available capacity. Based on a novel optical signal processing method,[1] we present and demonstrate an optically transparent add/drop node (ADN) that operates without use of a local transmitter. We show that it can be adjusted to be transparent to: the wavelength, the bit-rate (partly) and, as opposed to, e.g.,[2] the modulation format. To our knowledge, this is the first report on a modulation format independent ADN.

First, assume that the input of the ADN, depicted in Fig. 1, consists of a line-code, which has been constructed to avoid long runs of '0s' and '1s.' Usually these codes are referred to as runlength-limited (RLL) sequences[3] (e.g., Manchester line-code). The optical RLL input is directed to both the remaining optical ADN part and the node electronics. There it serves a dual purpose: (1) it contains the logical data sent to the node; (2) it is used, in combination with the 'add' information, to determine the switch-sequence. After alignment delay, an optical ($1 \rightarrow N$) coupler performs a copying operation of which the copies are delayed by $(0, 1, \ldots, N-1)$ time-slots, respectively. In each time-slot, which equals one line-code bit, one of the optical switches ($sw_0, sw_1, \ldots, sw_{N-1}$) is closed to forward the appropriate bit to the ADN output. Depending on the RLL line-code properties it can easily be shown that if the number of delayed branches, N, is greater than the longest possible run of '1s' or '0s' at the input, each arbitrary output can be created independent of the modulation format being applied (i.e., at least one '1' and one '0' are present before one of the switches in each time-slot). Hence, the amount of ADN-hardware can be traded-off against the maximum runlength in the RLL line-code.

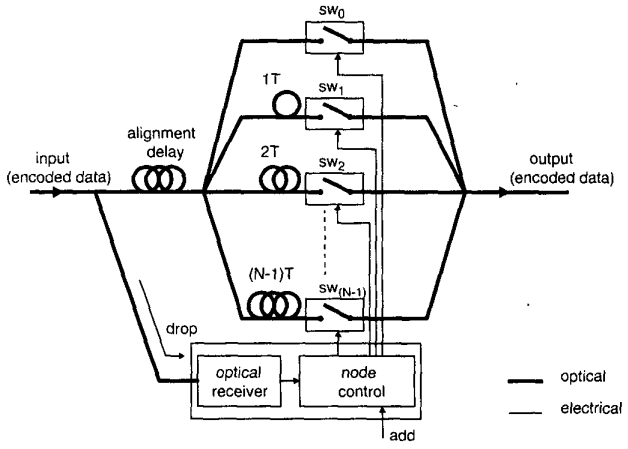

WM9 Fig. 1. General representation of the optically transparent add/drop node.

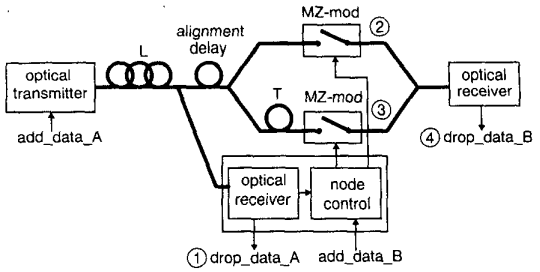

WM9 Fig. 2. Experimental and simulation set-up for demonstration of the add/drop node functionality. Bit-rate R_b = 622 Mb/s, L = 5 km and the bandwidth of the receive filter $BW = 0.7R_b$.

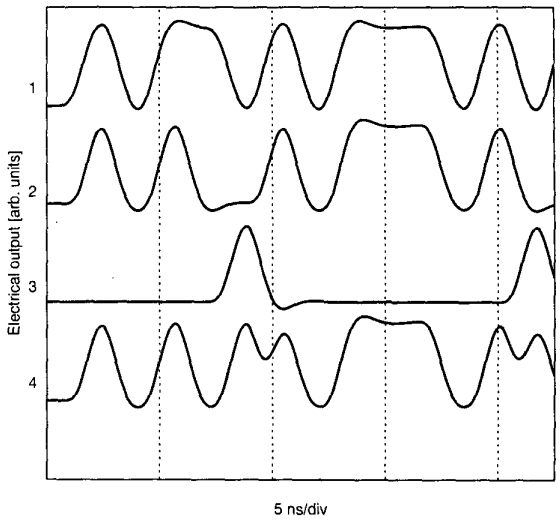

WM9 Fig. 3. Electrical representation of: (1) the dropped sequence A; (2) the output of sw_0; (3) the output of sw_1; and (4) the dropped sequence B.

In the special case that on-off keying (OOK) is employed, '0s' at the ADN output can also be created by interruption of the transmission path. In other words, the runlength of '0s,' L_0, should be restricted only. Based on this observation, we demonstrate the functionality of the ADN by means of a simulation of the set-up presented in Fig. 2. The add information of both A (01011010111010) and B (01010110111011) consists of a line-code, which restricts the runlength of '0s' to $L_0 \leq 1$ and, therefore, yields a minimal hardware configuration. In sequence are depicted in Fig. 3 (see also Fig. 2): (1) the dropped data A; (2) and (3) the output of the Mach-Zehnder switches (sw_0 and sw_1) before being combined; (4) the dropped data B. From these results it will be clear that the signal containing sequence A has been rearranged by the ADN to yield sequence B. Measurements of this set-up will be shown at the conference.

To summarize, we have presented a novel optically transparent add/drop node, which is able to drop data and simultaneously uses this encoded data for its add function. Hence, it does not need a local transmitter, it can process most modulation formats and can insert data at an equal or higher bit rate than the data that is dropped.

1. J. M. Rijnders and A. C. van Bochove, Signalprocessor, NL Patent Application NL1000682, filed June 28, 1995.

2. Y. Cai, R. M. Fortenberry, and R. S. Tucker, "Demonstration of Photonic Packet-Switched Ring Network with Optically Transparent Nodes," IEEE Photon. Technol. Lett. **6,** 1139 (1994).
3. K. A. Schouhamer Immink, "Runlength-Limited Sequences," Proc. IEEE, **78,** 1744 (1990).

WM10 3:48 pm

Novel self-healing configurations for broadband fiber-based access network architectures

Vijay K. Bhagavath, Harold Sobol, Ronald C. Menendez, Paul W. Shumate, Jr., *AT&T Bell Laboratories, Rm. 21-1D20, 1600 Osgood Street, N. Andover, Massachusetts 01845*

For video delivery and emerging critical information services requiring high survivability and availability in the access network (e.g., telecommuting, financial, and medical-related services), we investigate several optical-plus-electrical diverse-path and optical equipment protection configurations that significantly enhance the survivability and availability of broadband fiber-based access architectures.

Unprotected hybrid fiber/coax (HFC) and fiber supertrunk architectures are considered baseline cases for this study.[1] These architectures are modeled in an access area having a center horizontal mainleg street and 12 vertical sideleg streets, which contain a total of 384 living units.[1,2] In previous work, fiber-segment protection of two narrowband fiber-to-the-curb architectures were considered[2]; here we not only consider HFC and supertrunk fiber-segment protection, but also investigate the more challenging problem of HFC coaxial-segment and 1:16 optical equipment protection.

The baseline HFC architecture, illustrated in Fig. 1, consists of lightwave video transmission equipment at the central office and serving several access areas via 18-kft fiber trunks. Three video optical network units (V-ONUs) located on the mainleg (every V-ONU serves 128 homes), perform optical-to-electrical conversion prior to transmitting the video signal on coaxial buses that serve every sideleg. Four-way coax taps are present on the buses to deliver the video signals to every home via coaxial service drops. The baseline supertrunk architecture consists of a head-end station distributing programming to several central-office stations via 18-kft fiber trunks.

The self-healing fiber-trunk configuration for the HFC architecture (also applicable to the supertrunk case) is shown within the dotted box in Fig. 2. A 1:2 optical splitter in conjunction, with a 2 × 2 optomechanical switch, is situated at input ports of the V-ONUs in both access areas. The 2 × 2 switches in these access areas are interconnected via a vertical protection fiber, allowing the working fibers (WF-1 and WF-2) to serve the V-ONUs in both areas, thereby forming a "symmetrical" self-healing fiber trunk protection scheme.

Figure 2 also illustrates a self-healing fiber-trunk plus coaxial-feeder configuration. The four-way coaxial taps are placed with bidirectional "addressable-taps." The top and bottom through-ports of every addressable-tap can be electrically controlled by a protection controller to provide either a low loss (≈1–2 dB) or high insertion loss (≥50 dB) to the video

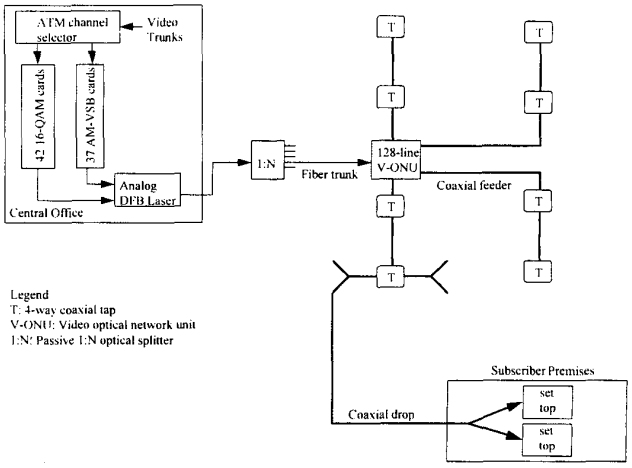

WM10 Fig. 1. Block diagram of the baseline hybrid fiber/coax access network architecture.

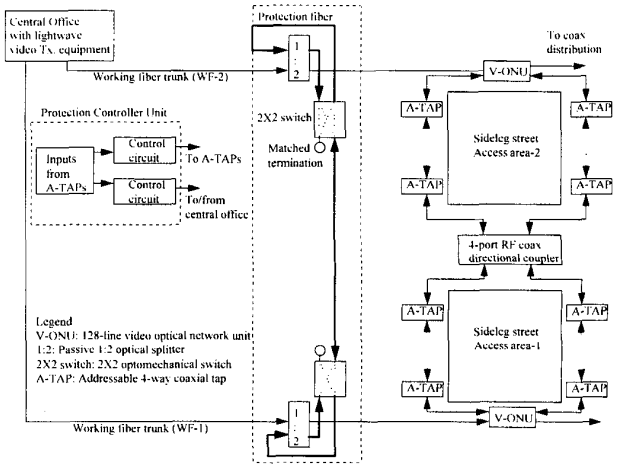

WM10 Fig. 2. Block diagram of the proposed self-healing configuration, which provides protection to the "fiber trunk" segment of the baseline hybrid fiber/coax and fiber supertrunk access network architectures.

signals incident at either port. A simple self-healing arrangement is formed by interconnecting the last addressable-taps in both sidelegs via a four-port directional coupler. In the event of a failure in either area, the protection controller provisions the last addressable-taps (in the sidelegs of both areas) to the low-insertion-loss state. This permits addressable-taps in the failed sideleg street to receive signals from addressable-taps in the adjacent sideleg.

A technical analysis is performed prior to reliability analysis to ensure that the self-healing alternatives achieve the specified requirements on system CNR, nonlinear distortion, and BER.[1] Generalized methodologies using probability analysis[1] and Markov modeling[3] are used to evaluate improvements in survivability and availability offered by the self-healing alternatives, relative to the baseline architectures.

Table 1 summarizes system requirements and reliability analysis results. The highlighted entries show that relative to unprotected baseline cases, the self-healing configurations achieve up to 70% increase in survivability and 55% decrease